Reynolds number dependence of plane jet development in the transitional regime

P. R. Suresh, K. Srinivasan, T. Sundararajan, and Sarit K. Das

Citation: Physics of Fluids (1994-present) **20**, 044105 (2008); doi: 10.1063/1.2904994
View online: http://dx.doi.org/10.1063/1.2904994
View Table of Contents: http://scitation.aip.org/content/aip/journal/pof2/20/4?ver=pdfcov
Published by the AIP Publishing

Reynolds number dependence of plane jet development in the transitional regime

P. R. Suresh, K. Srinivasan, T. Sundararajan, and Sarit K. Das[a)]
Department of Mechanical Engineering, Indian Institute of Technology Madras, Chennai 600036, India

(Received 21 June 2007; accepted 26 February 2008; published online 21 April 2008)

The transitional characteristics of plane turbulent jets have been investigated in the present study. Hot wire measurements have been performed for a jet issuing from a rectangular nozzle of aspect ratio 20, for Reynolds number varying in the range $250 \leqslant \mathrm{Re} \leqslant 6250$. In this range, the characteristics of flow development are found to be Reynolds number dependent, in contrast to the fully developed turbulent jets which show features independent of initial conditions such as inlet Re. For low Re jets, the jet spread is significantly influenced by the low frequency oscillations caused by shear layer instability. Large sized vortices are formed in the shear layers at the fundamental frequency of the instability, which lead to subharmonic low frequency oscillations due to vortex pairing and merger, at larger axial distances. Consequently, the far field flow structure of a low Re jet is dominated by large size vortices which give rise to a higher level of flow intermittency, larger entrainment of ambient fluid, and faster jet decay, as compared to high Re jets. Also, in the absence of finer scales and broader spectrum of eddies, the mean flow field achieves self-similar structure much ahead of the fluctuating components and fully developed turbulent flow characteristics are not observed, even in the far field. In high Re jets, on the other hand, the vortex break-up processes also simultaneously occur along with vortex pairing and merger. Therefore, energy transfers to a broad spectrum of scales and finer scales are observed even in the near field of the jet. Although the achievement of self-similarity for the mean field is slightly faster than that for the fluctuating components, turbulence also attains a fully developed state at about a nondimensional axial distance of 20. The associated probability density functions of the fluctuating components evolve into Gaussian profiles, implying isotropic turbulence. Due to the dominance of finer scales, the overall entrainment level is less and decay is slower for a high Re jet. © *2008 American Institute of Physics*. [DOI: 10.1063/1.2904994]

I. INTRODUCTION

In spite of the voluminous research literature available on turbulent free jets issuing from rectangular nozzles, there are still some fundamental aspects which require detailed attention. For instance, in rectangular jets of large aspect ratio, primarily, planar spreading occurs in the near field. In the thin shear layers outside the jet potential core, disturbances tend to grow, causing fluctuations in the flow field. Entrainment of the ambient fluid occurs into the shear layer by viscous action, which in conjunction with the growth of instability, leads to the roll up of fluid in the form of vortices. The vortices in turn, enhance mixing within the jet and eventually contribute to flow transition from laminar to turbulent regime. Far away from the nozzle exit, the jet loses memory of the nozzle cross sectional shape and the flow asymptotically attains the self-similar profile of a turbulent round jet. The turbulent flow fluctuations also evolve as the jet spreads with an increase in axial distance; the rates of evolution of the mean flow field and the turbulent fluctuations, however, are quite different. The present study focuses attention on the evolutionary features of mean flow and turbulent fluctuations with axial distance and investigates the effect of jet flow Reynolds number (Re) on such phenomena.

Many studies have so far been conducted for establishing the general features of plane jets.[1–3] Brown *et al.*[4] observed that the interaction region between the two opposite shear layers of a plane jet extends up to $x/d=20$, where x is the axial distance and d is the height of the nozzle. Namer and Otugen[5] studied plane jets between Re of 1000 and 7000 and obtained correlations for their spread rates. Instability waves generated from the nozzle lips have been initially found to be two dimensional in nature, especially in the case of laminar shear layers which roll up in the form of coherent structures.[6,7]

There is a substantial amount of work describing the interactions of the shear layer, its structural development, and classification of different regions, mostly for high Re jets.[8–11] Weir *et al.*[3] studied interacting turbulent shear layers in a plane jet. It was observed that although the two shear layers merge at around $6d$, self-preservation is attained beyond $20d$. Gutmark and Wygnanski[2] found turbulent plane jets to be self-preserving for $x/d>40$. Experiments conducted for rectangular jets of aspect ratio of 16.5 by Krothapalli *et al.*[12] revealed that the flow field is characterized by three distinct regions, i.e., a potential core region followed by a two dimensional region and, finally, an axisymmetric

[a)]Author to whom correspondence should be addressed. Electronic mail: skdas@iitm.ac.in.

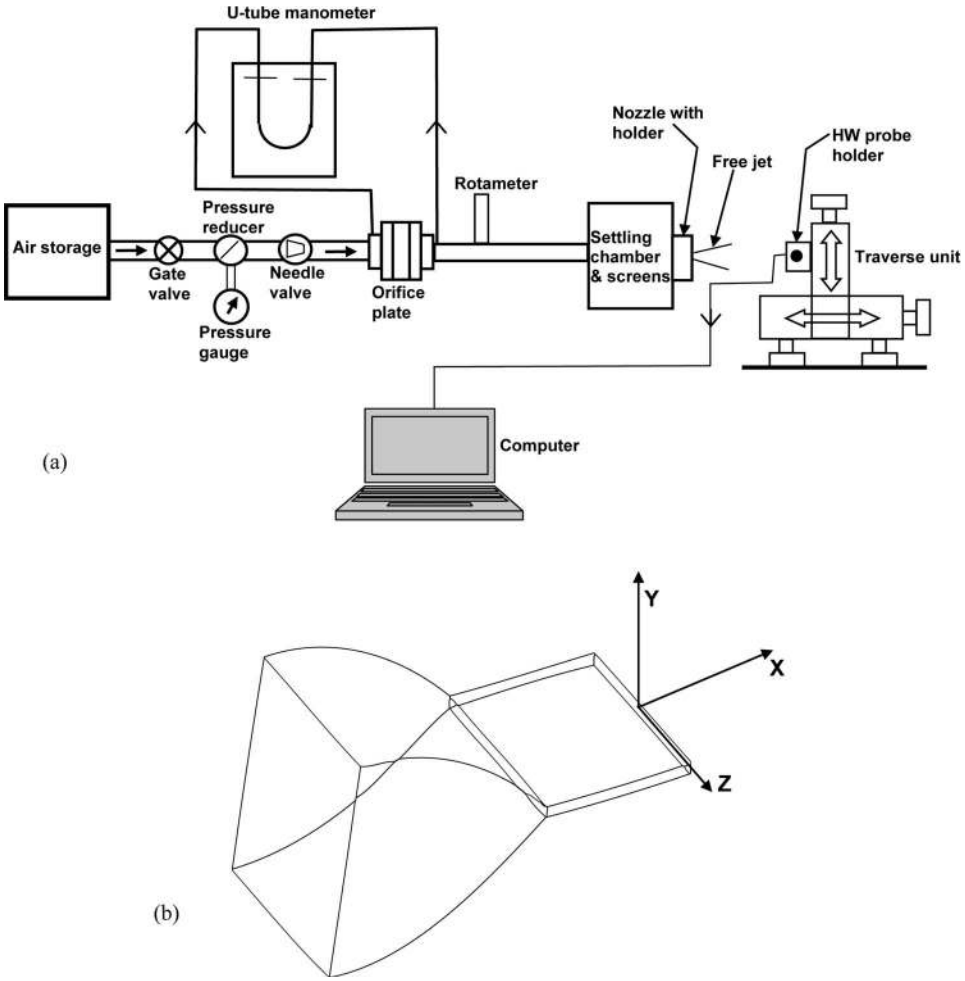

FIG. 1. Schematic of the experimental setup.

region. Thomas and Chu,[13] in a study of plane jet at a moderate Re of 8300, used a low level acoustic excitation to organize the initial instability waves and studied their downstream evolution. Several authors have looked at the effects of initial conditions at the jet inlet upon the spreading characteristics of a turbulent jet.[14–17] Tam and Norum[18] concluded that in a supersonic large aspect ratio impinging jet, several tones are produced by a feedback loop comprising upstream propagating acoustic waves and downstream propagating instability waves.

From the above literature survey, it is clear that most of the existing studies correspond to the fully turbulent Reynolds number regime and very few studies are available in the transitional Reynolds number range. Also, the evolutionary features of the mean flow and fluctuating flow components and their effects on jet spread have not been adequately addressed in the earlier studies. The present work aims to provide information on the effect of Reynolds number on the development of self-similarity for both the mean and fluctuating quantities and the associated flow structure development. The less explored Re range of 250–6250 is studied (where Re is the Reynolds number which is defined as $U_0 d/\nu$, U_0 is the jet exit velocity, d is the smaller dimension of the rectangular jet, and ν is the kinematic viscosity of air) and the flow features are analyzed with the help of mean and turbulence measurements, spectral analysis of the turbulent fluctuations, and the probability distributions of fluctuations. The evolution of turbulence and the asymptotic approach to isotropic turbulence are also highlighted.

II. EXPERIMENTAL SETUP

A schematic of the experimental setup is shown in Fig. 1. Compressed air stored in a vessel is admitted through a pressure regulator into a settling chamber of 300 $\times 300$ mm^2 cross section and 600 mm length. A calibrated orifice meter is used to measure the air flow rate, based on which the average nozzle exit velocity is calculated. A honeycomb structure made of straws and two layers of very fine mesh is employed in the settling chamber to reduce the turbulence level of the incoming flow. This turbulence management system effectively brings down the turbulence intensity to a low value of 0.5% at the nozzle exit for the range of average jet inlet velocities 2.1–51.9 m/s (i.e., Re ranging from 250 to 6250).

The shape of the jet nozzle is known to play an important role in the near field development of a free jet flow. In the present experiments, a convergent nozzle of contraction ratio 20 with a fifth order polynomial profile has been used to generate a smooth attached flow. A parallel channel of length adjustable up to 150 mm is attached to the nozzle to achieve the desired laminar inlet velocity profile for the jet. When an

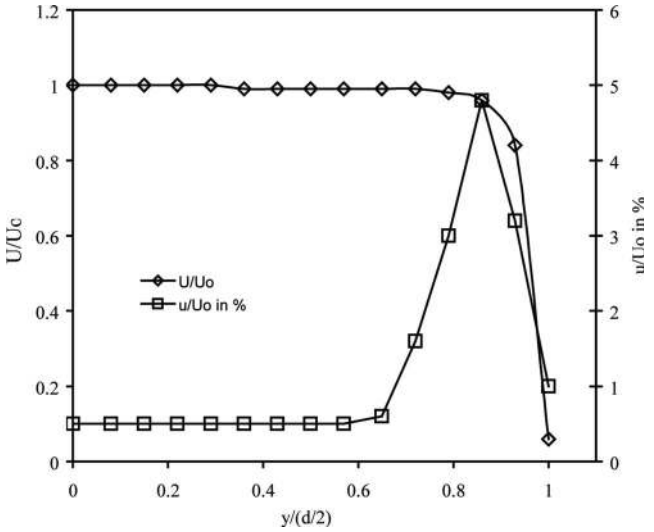

FIG. 2. Boundary layer at the exit of the nozzle for Re=6250, x/d=0.5.

adequate straight lip is not provided following the contraction, the boundary layer can deviate from the Blasius profile even in the laminar regime.[6] The final slot dimensions of the nozzle are 40 mm width (W) and 2 mm height (d), providing an aspect ratio of 20. The nozzle has been designed using numerical flow simulation and manufactured by the electro-discharge machining process. The slot has sharp edges to prevent nonuniformities at the nozzle exit and to provide precise initial conditions for the jet inlet.

Mean and fluctuating velocities have been measured using DANTEC 90N10 hot wire anemometer, using a 5 μm diameter, 1.5 mm long wire made of platinum coated tungsten. The hot wire anemometer is calibrated using a pitot tube and a micromanometer (Furness Control-FCO12) with an accuracy of $\pm 1\%$ of the reading and linearity better than 1% of the reading. The voltage-velocity calibration graph is fitted with a power law form $E=A+BU^n$, where A and B are constants. The wire probe is cleaned in acetone solution after every 3 h exposure to air flow for removing any possible contamination and then recalibrated. Correction is applied to the calibration curve in order to account for any variations in the ambient temperature. The data acquisition system is a 12 bits analog to digital converter. The mean and rms values are sampled at the rate of 1 kSa/s (kilosamples per second) for a sampling time of 30 s. For the measurement of power spectra of velocity fluctuations, the maximum sampling frequency used was 50 kHz at the highest Reynolds number. The probe was operated at an overheat ratio of 1.8. Four traces of 2, 62, and 144 points were averaged for each spectrum. For each data trace, a Blackman window and an averaging routine were used with 62 overlapping data segments of 1024 points.

Uncertainty in the velocity measurement is threefold: Uncertainty from calibration, curve fitting, and signal conditioning. The overall uncertainty in mean velocity is estimated to be less than 1.2% except for the two lower Re cases (Re=250 and 550), where it increases up to 2%. The turbulent fluctuations have an uncertainty of 3.1% based on the estimate from standard deviation. The estimate of frequency has a maximum uncertainty of ± 6.1 Hz. The propagation of uncertainty in derived quantities is calculated by the method of propagation.[19] Accordingly, the turbulence intensity, Reynolds number and Strouhal number have uncertainties of 3.8%, 1.33%, and 1.11%, respectively.

TABLE I. Inlet conditions of the jet (x/d=1 mm).

Re	δ (mm)	Δ (mm)	H
250	0.155	0.073	2.12
550	0.145	0.067	2.16
1100	0.139	0.062	2.24
2000	0.115	0.045	2.56
4000	0.11	0.0424	2.59
6250	0.0709	0.0265	2.68

In order to fully understand the evolution of the jet flow features, it is necessary to measure the mean velocity profile and its characteristic length scales such as displacement and momentum thicknesses and the shape factor of the boundary layer at the jet inlet. In the present study, mean and fluctuating velocity components (U and u) have been measured at an axial distance of 1 mm from the nozzle exit at different Reynolds numbers and the jet inlet profile for Re=6250 is plotted in Fig. 2. For this case, the displacement thickness (δ) obtained by numerical integration is 0.0709 mm and momentum thickness (Δ) is 0.0265 mm. The ratio of the displacement to momentum thickness, known as the "shape factor," is found to have a value of 2.68. This is close to the value of 2.5 obtained for the Blasius velocity profile in laminar boundary layer flow over a flat plate. The values of δ and Δ for various Reynolds numbers are summarized in Table I. The turbulence intensity has a low value (less than 0.5%) in the core region and attains a peak value in the shear layer. These profiles illustrate that at the nozzle exit plane, a nearly uniform laminar velocity profile prevails for the Reynolds number cases investigated in the present work.

III. RESULTS AND DISCUSSION

A. Near field and far field flow features

The development of mean flow in the near field is shown in Fig. 3. In the figure, U_0 and U_c denote the jet exit velocity and centerline velocity, respectively. At low Reynolds number (Re=250 and 550), the mean centerline velocity decay is relatively slower than at higher Reynolds numbers. Since turbulent kinetic energy generation depends on the mean velocity gradients, higher turbulence generation in the shear layer increases mixing with the ambient fluid (i.e., greater level of entrainment), which results in faster decay at higher Re in the near field. Consequently, the potential core length is also observed to slightly decrease with Reynolds number, particularly at higher Re values (Fig. 3). Namer and Otugen[5] found a decrease in potential core length from 4d to 2d, when Re is increased from 1000 to 7000.

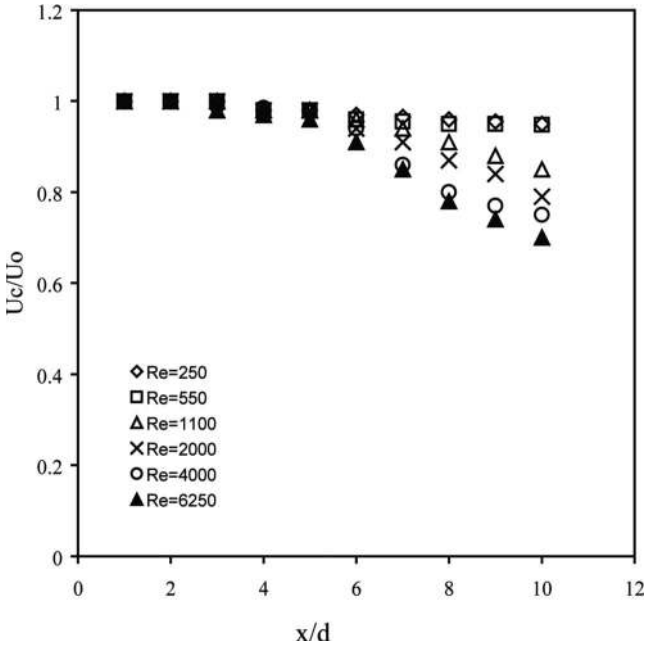

FIG. 3. Development of mean velocity in the near field.

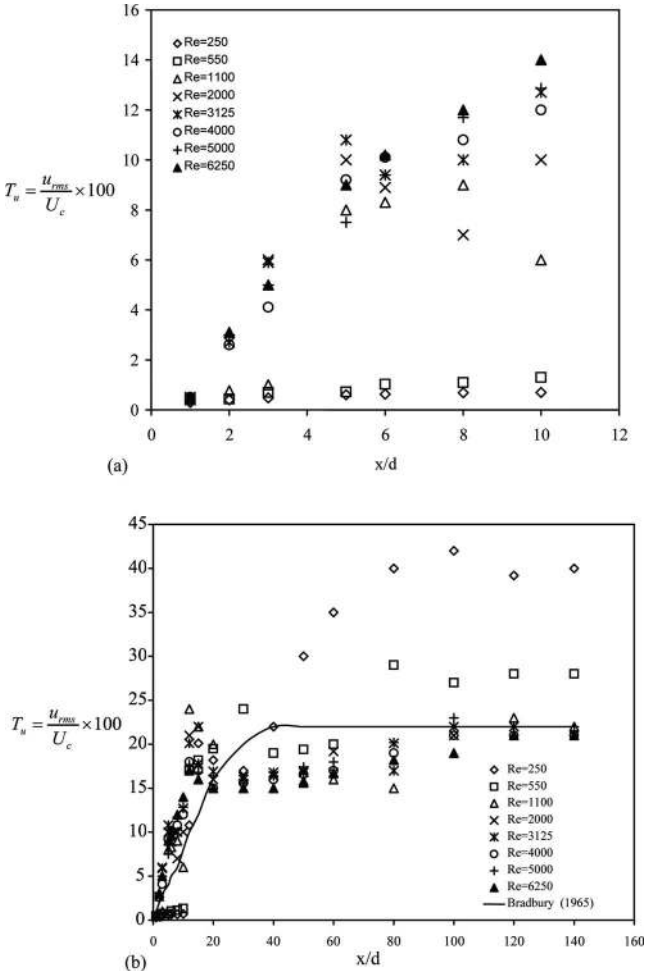

FIG. 4. Variation of turbulence intensity. (a) Near field; (b) far field.

The growth of turbulence in the near and far field regions at different Reynolds numbers is shown in Figs. 4(a) and 4(b). Figure 4(a) is a zoomed picture of Fig. 4(b) for the region $0<x/d<12$ shown to more clearly illustrate the growth of turbulence intensity in the near field. The reason for the slow increase of turbulence intensity T_u in the low Re cases is the existence of an initial "laminar length," where the turbulent fluctuations are extremely small. For low Re jets (Re<1100), in the near region (for $x/d\leqslant 20$), the flow field essentially remains laminar. The turbulence intensity shows an initial linear growth up to a value of 6% [Fig. 4(a)] for Reynolds numbers greater than or equal to 2000. This value was observed as 4% by Sato and Sakao.[20] The observed peak and dip in the turbulence intensity values (T_u) between $x/d=6$ and 10 arise due to shear layer interactions after the potential core.

Axial evolution of turbulence intensity at different Reynolds numbers is shown in Fig. 4(b). Far field turbulence intensity values are higher for Re values of 250 and 550 and these do not approach self-similar behavior even at large axial distances of $x/d\approx 140$. For higher Re values, the turbulence intensity approaches an asymptotic fully developed state which is independent of Re or axial distance. A higher turbulence level for low Reynolds number flow (as compared to that at high Re) has been reported by Peterson and Bayazitoglu[21] for an axisymmetric jet, similar to the present plane jet case. As explained later with the help of spectral data, the fluctuations of high amplitude noted at low Re are contributed by large sized vortices lying in a narrow frequency band, which do not correspond to a fully developed turbulent state. They rather give rise to an essentially laminar flow with a high level of intermittency. It is seen that the turbulence intensity peaks in the range $5<x/d<20$ for high Re cases. This is possibly due to the interaction between the two mixing layers growing from the opposite sides. Beyond $x/d=80$, the turbulence intensity attains an asymptotic value of 22% in close agreement with the value obtained by Bradbury[1] for a jet at Re=30 000.

It was suggested by Krothapalli *et al.*[12] that the presence of a large centerline peak in the axial velocity fluctuation (u) in the interaction region may depend on the initial boundary layers at the nozzle lip being laminar or turbulent. In the present case, such a shear layer interaction region with peak u value occurs between $5d$ and $15d$, as seen from the turbulence intensity profiles plotted in Fig. 4(b). The high velocity fluctuations can be attributed to large scale double roller structures rather than Kelvin–Helmholtz vortices which usually occur only in the near field.[10] The peak intensity value in the interaction region is seen to decrease with the increase in Reynolds number. Spectral studies described later show that this region for a low Re jet is dominated by more organized coherent structures caused by shear layer instability. More vigorous and intermittent inclusions of ambient fluid can produce large fluctuations at low Re. When Re is increased, the fluctuations essentially become three dimensional, less coherent, and correspond to finer scales in the interaction region and, hence, the maximum value of T_u attained is lower.

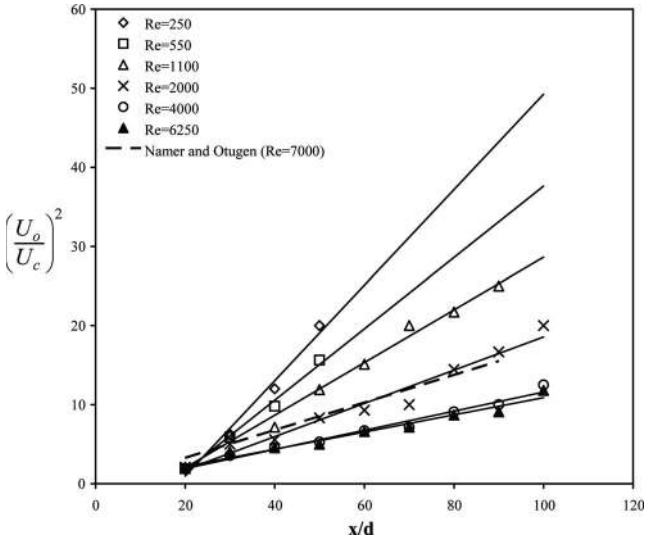

FIG. 5. Variation of inverse mean velocity square with axial distance.

B. Jet spread rate and flow visualization

Large Plexiglas side plates have been used in the present work to facilitate two dimensional spreading of the jet by preventing lateral entrainment of ambient air. The conventional measures of jet spreading and velocity decay give the following relations in the fully developed region:

$$\left(\frac{U_0}{U_c}\right)^2 = K_{1u}\left(\frac{x}{d} - C_{1u}\right), \tag{1}$$

$$\frac{b_u}{d} = K_{2u}\left(\frac{x}{d} - C_{2u}\right), \tag{2}$$

where b_u is the jet half-width, U_c is the local centerline velocity, U_0 is the mean nozzle exit velocity, and K_{2u} is the jet spread rate. Also, C_{1u} and C_{2u} are the locations of virtual origin for the mean velocity decay and jet half-width, respectively. Axial variations of the inverse velocity square $(U_0/U_c)^2$ are shown in Fig. 5. The results of Namer and Otugen[5] for Re=7000 are also shown in the figure for comparison. For Re<1100 and $x/d>40$, the mean velocity decay is very fast. In fact, for such low Re situations, fluctuations become comparable to the mean velocities in the far field [Fig. 4(b)] and the entrained mass flow rate is significant compared to the jet inlet flow rate, even at moderate values of x/d. These trends can be attributed to the dominance of large sized vortices in the far field of a low Re jet.

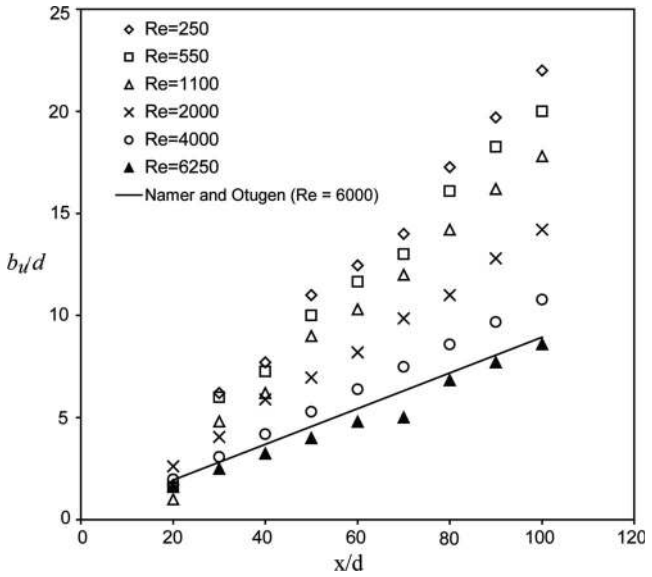

FIG. 6. Variation of half-width with axial distance.

TABLE II. Virtual origins and spread rate of half-width and centerline decay.

Re	K_{1u}	C_{1u}	K_{2u}	C_{2u}
250	0.6	18.5	0.24	8.1
550	0.45	16.6	0.22	7.11
1100	0.33	14.1	0.2	9.35
2000	0.21	11.71	0.14	1.2
4000	0.12	4.25	0.11	2
6250	0.11	−0.08	0.086	3.05

The y locations at which the mean velocity U becomes half of the centerline velocity U_c are determined as the values of jet half-width. Variation of dimensionless half width (b_u/d) with axial distance is plotted in Fig. 6. Results of Namer and Otugen[5] for Re=6000 are also shown in the figure for comparison. The slope of half-width K_{2u} $(=db_u/dx)$ is 0.086 for this study at Re=6250 which is quite close to the value of 0.10 obtained by Thomas and Goldschmidt[11] using a long approach channel nozzle at Re=6000. The mean velocity decay constant (K_{1u}) obtained in the present study is 0.11. The variations of the developed jet flow parameters K_{1u}, K_{2u}, C_{1u}, and C_{2u} with Re are shown in Table II. Both the slopes K_{1u} and K_{2u} show a decreasing trend with Re in general and attain asymptotic values of around 0.1 at higher Reynolds

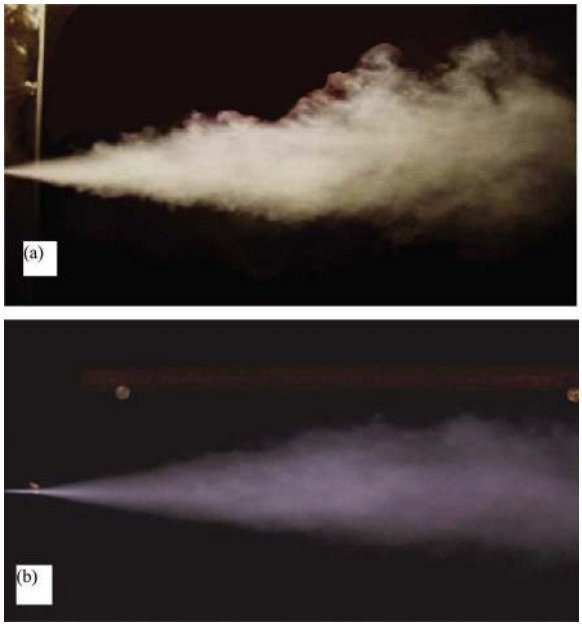

FIG. 7. (Color online) Reynolds number dependence of a plane jet. (a) Re=250; (b) Re=6250.

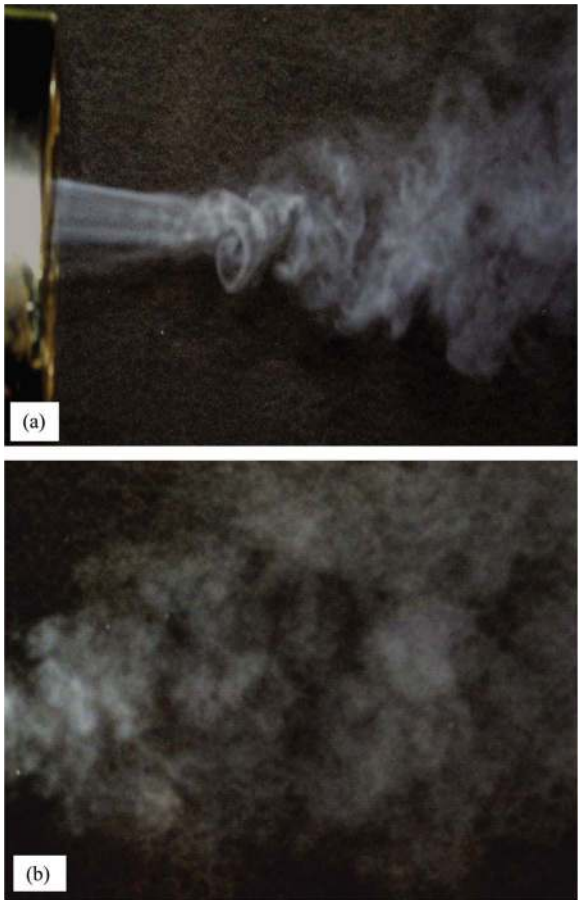

FIG. 8. (Color online) Spatial development of a jet at Re=250. (a) Near field spread; (b) far field.

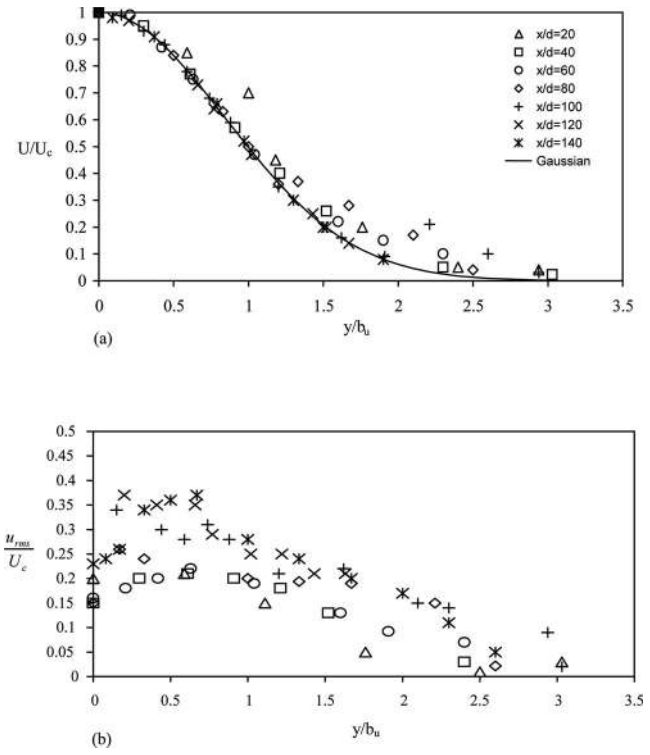

FIG. 9. Radial variation of velocity field at Re=250. (a) Mean velocity; (b) fluctuating velocity.

numbers. It is evident that the jet spread rate decreases with Re due to the dominance of finer scales in high Reynolds number jets. The virtual origin C_{1u} decreases with the increase in Re showing a shift of origin toward the nozzle side. The virtual origin C_{2u} on the other hand increases at higher Re (Re$>$2000) implying a shift away from the nozzle. These changes can be attributed to the variations in the boundary layer thickness at the nozzle exit with the increase in Re. Thus, the low Re jets (Re$<$2000), in general, exhibit trends which are significantly different from the trends for high Re jets.

Flow visualization with smoke has been carried out using a digital camera, with exposure times of the order of a second, as shown in Figs. 7 and 8. At low Reynolds number, the photographs show dominance of large scales in the outer shear layer zone [Fig. 7(a)]. This is the active mechanism in a low Re jet by which entrainment takes place due to the Biot–Savart induction process. Comparing this with the photograph of a high Re jet at Re=6250 [Fig. 7(b)], it is observed that large scales are absent in the outer shear layer. Consequently, ambient air entrainment decreases, leading to reduction in the jet spread rate with increasing Re. Thus, flow visualization photographs qualitatively support the trends obtained from hot wire anemometer data. Photographs of the near and far field developments of a low Reynolds number jet (Re=250) are shown in Fig. 8. The near field development shows shear layer stretching, resulting in the formation of vortices. This is the chief mechanism by which jets engulf fluid from the ambient. The photograph of far field flow structure in a low Re jet is shown in Fig. 8(b). This shows adjoining regions of smoke and ambient air throughout the jet cross section, implying that intermittent excursion of ambient fluid occurs right up to the jet centerline. In other words, large levels of flow intermittency prevail in the far region of a low Re jet.

C. Self-similarity of mean and fluctuating quantities

Variations in the transverse direction, of the dimensionless mean and fluctuating axial velocity components U/U_c and u/U_c, are plotted in Figs. 9–11 in order to study the self-similar behavior of these quantities. The Gaussian curve $U/U_c=\exp\{-C(y/b_u)^2\}$ with $C=0.7$ is also plotted in the figures for the sake of comparison. The mean velocities are self-similar in lower Re cases for $x/d>20$, particularly close to the jet midplane [Fig. 9(a)]. At the jet periphery, for $y/b_u>1.5$, similarity is poor probably because of the shear layer instability mechanisms at play and the plane to axisymmetric jet transition. At the higher Reynolds numbers of 2000 and 6250 [Figs. 10(a) and 11(a)], attainment of self-similarity for the mean velocity occurs earlier than in the case of low Re jets. The outer shear layer regions exhibit minor deviations from similarity for the mean velocity profile of Re=2000, for the same reasons mentioned above.

Turbulence intensity profiles plotted in Figs. 9(b), 10(b), and 11(b) exhibit a stronger Reynolds number dependence for the attainment of self-similarity. At Reynolds numbers between 250 and 2000, turbulence intensity values are very much scattered and do not show any trend toward self-

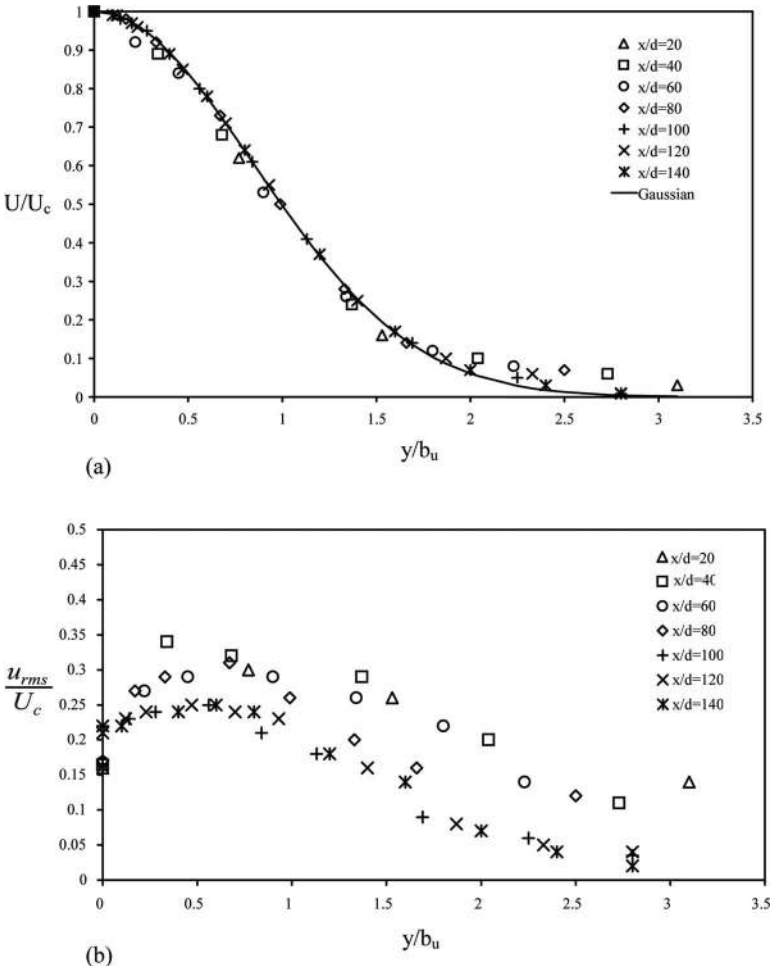

FIG. 10. Radial variation of velocity field at Re=2000. (a) Mean velocity; (b) fluctuating velocity.

preservation [Figs. 9(b) and 10(b)]. Moreover, turbulence intensities attain relatively higher values in the central part of the jet with $u/U_c \sim 0.35$. At higher Reynolds numbers (Re=6250), attainment of self-similarity for the turbulence intensity is confirmed by the collapse of the data onto a single curve [Fig. 11(b)]. From the plots presented here, it is clear that mean quantities attain self-similarity earlier than fluctuating quantities. Since energy transfer occurs from the mean flow to the turbulent eddies, some time is required for the fluctuating quantities to attain self-similarity after the mean flow becomes self-similar, especially in cases where the flow is dominated by large sized eddies (i.e., low Re). Hence, it can be concluded that for plane jets issuing at low Reynolds numbers, self-similarity is attained by the mean and fluctuating quantities at different locations. Only at higher Reynolds numbers, both mean flow and turbulence intensities tend to achieve self-similarity almost simultaneously. This can be attributed to the early evolution of vortex structures and faster approach toward isotropic turbulent state, in the cases of high Re jet flows.

D. Spectral analysis

The contrasting trends of jet spread seen in low Re and high Re jets and also in the near field and far field regions can be better explained by having a closer look at the spectral data for the associated velocity field. Here, power spec-

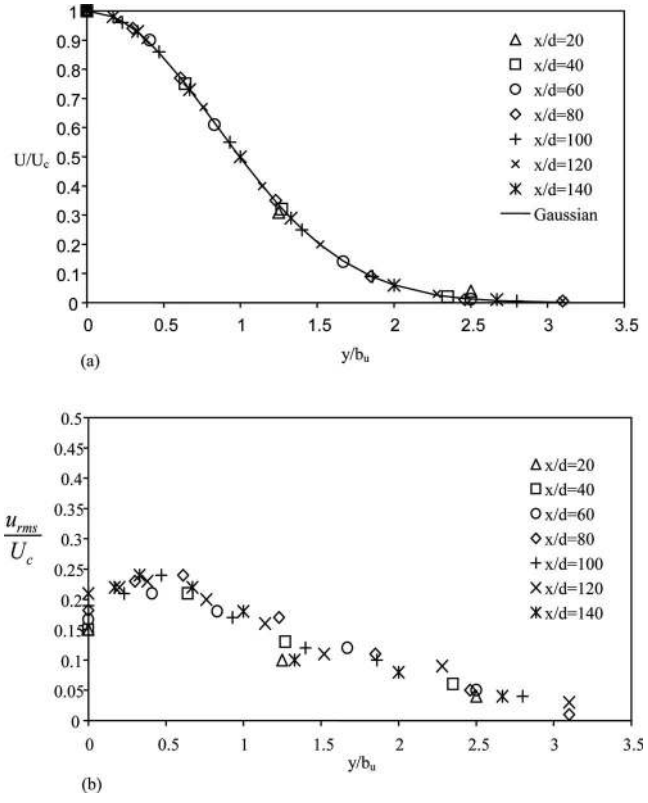

FIG. 11. Radial variation of velocity field at Re=6250. (a) Mean velocity; (b) fluctuating velocity.

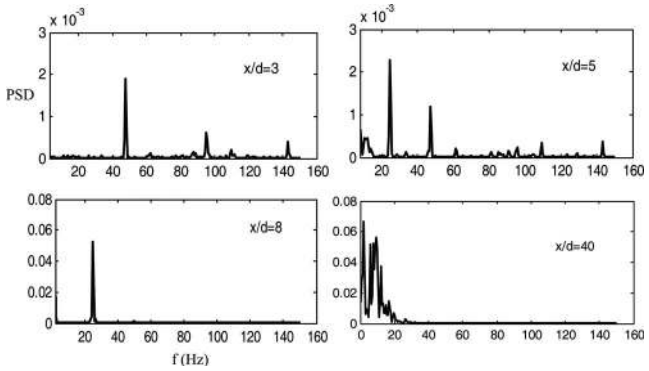

FIG. 12. Variation of spectra along the centerline for Re=250.

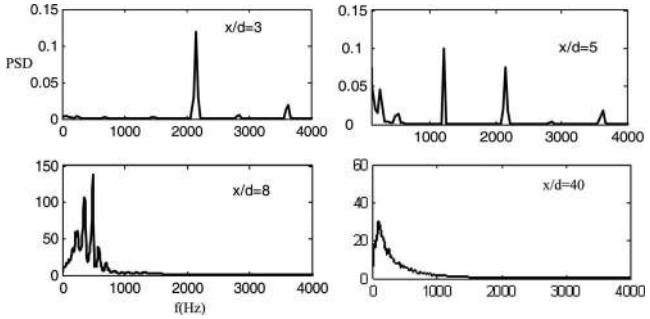

FIG. 14. Variation of spectra along the centerline for Re=1100.

tral density of velocity fluctuations obtained through fast Fourier transform along the jet centerline at different axial locations are systematically presented and discussed.

When a laminar shear layer becomes unstable, velocity fluctuations increase in amplitude resulting in the roll up of the shear layer into a train of spanwise rectilinear vortex elements. Such vortex formation gives rise to discrete frequency components in the spectra of velocity fluctuations, in the region close to the nozzle exit. Even a small inequality in the size or strength of adjacent vortices will induce them to roll around one another, forming an equivalent larger vortex. This pairing process for vortices has been observed by earlier researchers in circular as well as plane jets.[6] Vortex pairing is reflected as frequency halving in the spectrum.

Interaction of the two shear layers and the vortex-pairing processes in a plane jet with an initial top hat profile is distinctly different from that of a fully developed velocity profile.[6] In the present case, it is expected that frequency halving as a result of pairing of vortices may immediately occur beyond the potential core, when the shear layer interactions become more intense. For low Re jets of Re=250, 550, and 1100, interaction and frequency halving are seen to occur beyond the potential core in Figs. 12–14. In Fig. 12 (Re=250), the power spectrum exhibits a fundamental vortex formation frequency of 48 Hz at $x/d=3$. The subharmonic with $f=24$ Hz (where f is the frequency) is observed at $x/d=5$ which then grows in amplitude and finally develops into several subharmonic components at larger axial distances ($x/d\approx 40$). Similarly for Re=550, the fundamental frequency is 342 Hz at $x/d=3$ (Fig. 13). At the end of the potential core ($x/d=5$), the subharmonic of 171 Hz dominates over the fundamental component. Broadening of the spectrum in the subharmonic range is seen for still larger axial distances. Similar features are observed for Re=1100 (Fig. 14) also with a fundamental frequency of $f\sim 2000$ Hz. Interestingly, vortex breakup processes, which produce finer scales, seem to be absent in the low Re jets, even in the far field. At a high Re such as 6250, no discrete peaks are seen in the near field (Fig. 15). Finer scales appear at small axial distances and a fully developed spectrum is also attained at an earlier axial distance ($x/d=20$). The spectral plots confirm the earlier observation that the length required for transition to fully developed turbulence decreases with an increase of Reynolds number.

Based on the dominant frequency of the spectrum, one can estimate the corresponding eddy Reynolds number from a scale analysis as follows. Taking the eddy length scale as $d/2$ (shear layer thickness at the end of potential core) and velocity scale as $fd/2$, where f is the dominant frequency, the eddy Reynolds number Re_e is obtained as $fd^2/4\nu$, where ν is the kinematic viscosity. This estimate illustrates that the eddy Reynolds number is $O(10)$ or less, for the jet Re values of 250 and 550. For jet Re=2000, it becomes $O(100)$. At such high eddy Reynolds numbers, the vortex breakup will also become important, while the breakup processes may be nearly absent for the low Re jets. The above scale analysis explains the reasons for the near absence of finer scales in the low Re jets. Consequently, the low Re jets are dominated by large size eddies throughout the length, which results in greater entrainment and jet decay.

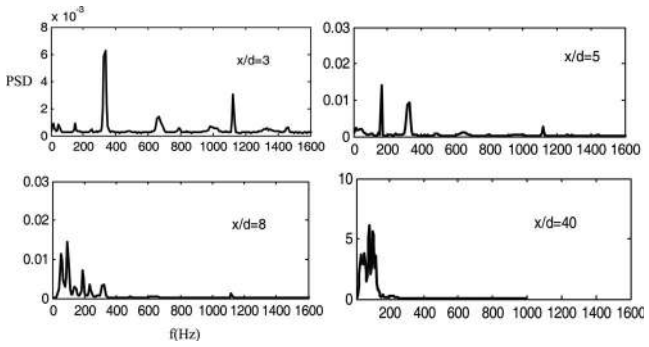

FIG. 13. Variation of spectra along the centerline for Re=550.

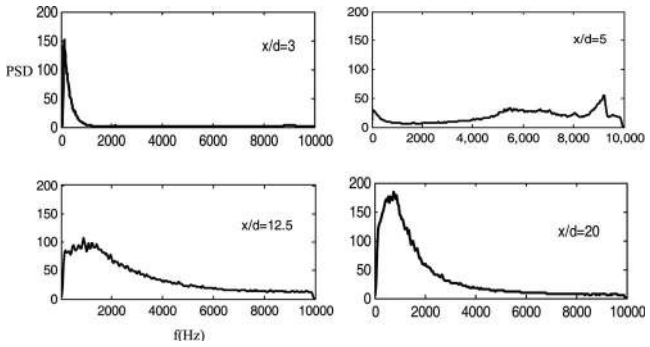

FIG. 15. Variation of spectra along the centerline for Re=6250.

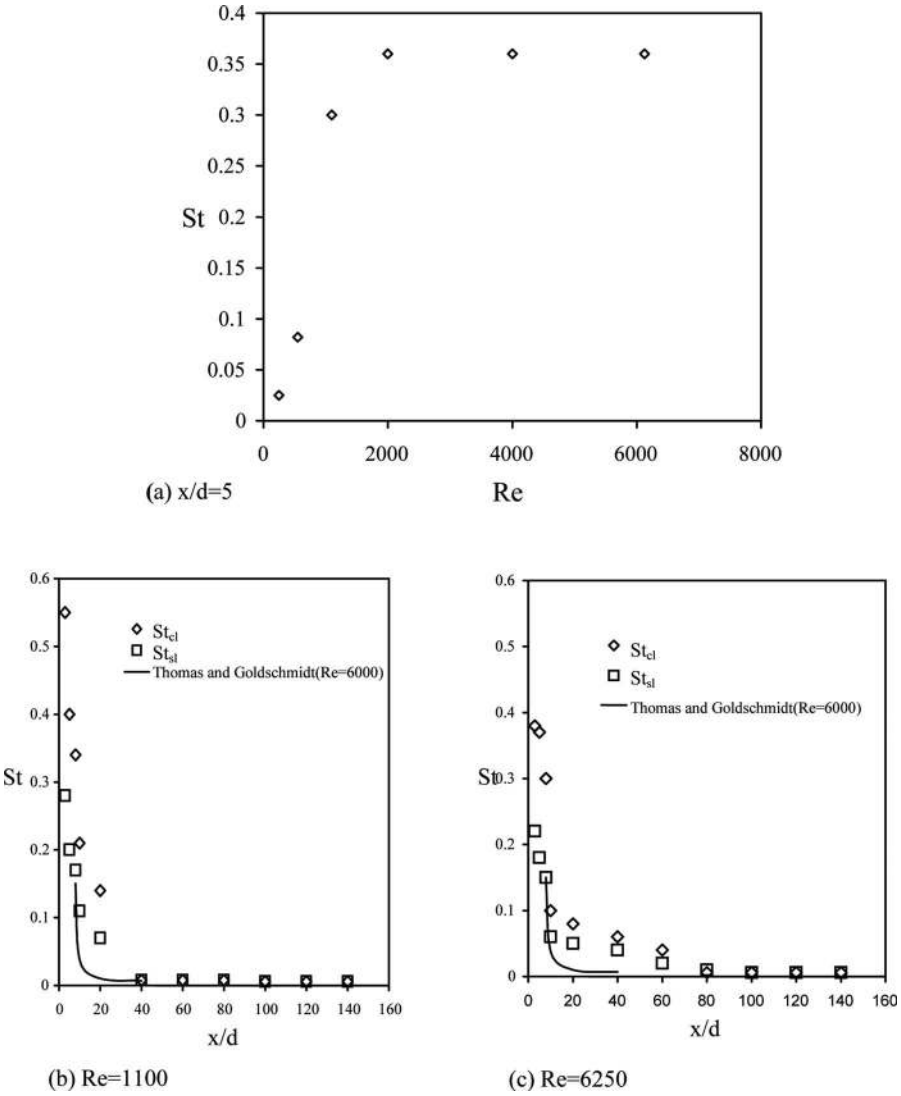

FIG. 16. Variation of Strouhal number (a) with Reynolds number. (b) With axial distance along centerline; (c) with axial distance in shear layer.

The dominant frequency is taken from the power spectra plots at $x/d=5$ (Figs. 12–15) and the corresponding Strouhal number (St) is estimated using jet height and inlet velocity, ($\mathrm{St}=fd/U_0$). The values of St for Re=250, 550, and 1100 turn out to be 0.025, 0.082, and 0.3, respectively. For Reynolds numbers of 2000 and higher, the asymptotic value of Strouhal number approaches 0.36 [Fig. 16(a)] which is close to the value of 0.3 obtained by Namer and Otugen.[5] At high Reynolds numbers, i.e., Re>2000, Strouhal number tends to become independent of Reynolds number.[8,22] Since the growth of shear layer with distance is slow at higher Reynolds numbers, disturbances due to vortex formation and entrainment do not penetrate to the centerline in the near field. Hence, the number of vortex rings formed per unit time remains unchanged (thereby resulting in a constant value of St) at higher Reynolds numbers.

Variations of St (based on the dominant frequency component in the spectrum) with axial distance are plotted in Figs. 16(b) and 16(c), for Re values of 1100 and 6250. Strouhal number has been calculated along the jet centerline and also at the location where the mean velocity becomes half of the local centerline velocity. These have been termed as "centerline Strouhal number" ($\mathrm{St_{cl}}$) and "shear layer Strouhal number" ($\mathrm{St_{sl}}$), respectively. It is clear that the centerline Strouhal number ($\mathrm{St_{cl}}$) is higher than the shear layer Strouhal number ($\mathrm{St_{sl}}$) near the nozzle; however, beyond a certain axial distance, the two Strouhal numbers approach a single value. For lower Re jet [Fig. 16(b)], convergence of the two Strouhal number values is observed at $x/d=40$, while at Re=6250, convergence occurs at around $x/d=80$. Similar Reynolds number dependence of Strouhal number convergence was observed by Thomas and Goldschmidt[11] for a jet issuing from a long channel. The earlier collapse of $\mathrm{St_{cl}}$ and $\mathrm{St_{sl}}$ in the low Re jet flow of the present study can be explained in terms of the faster shear layer growth at lower Re. Occurrence of different instability modes and their Re dependence have been discussed by Tam and Thies[23] and Ho and Huerre.[24]

In all the cases studied, the power spectra are initially discrete; they gradually become broadened with axial distance; however, a fully developed turbulent flow is eventually achieved only at higher Reynolds numbers. It is evident that the dominant part of the spectrum shifts toward lower frequencies (larger eddies) as a result of interaction between the dominant peaks and a redistribution of energy. The en-

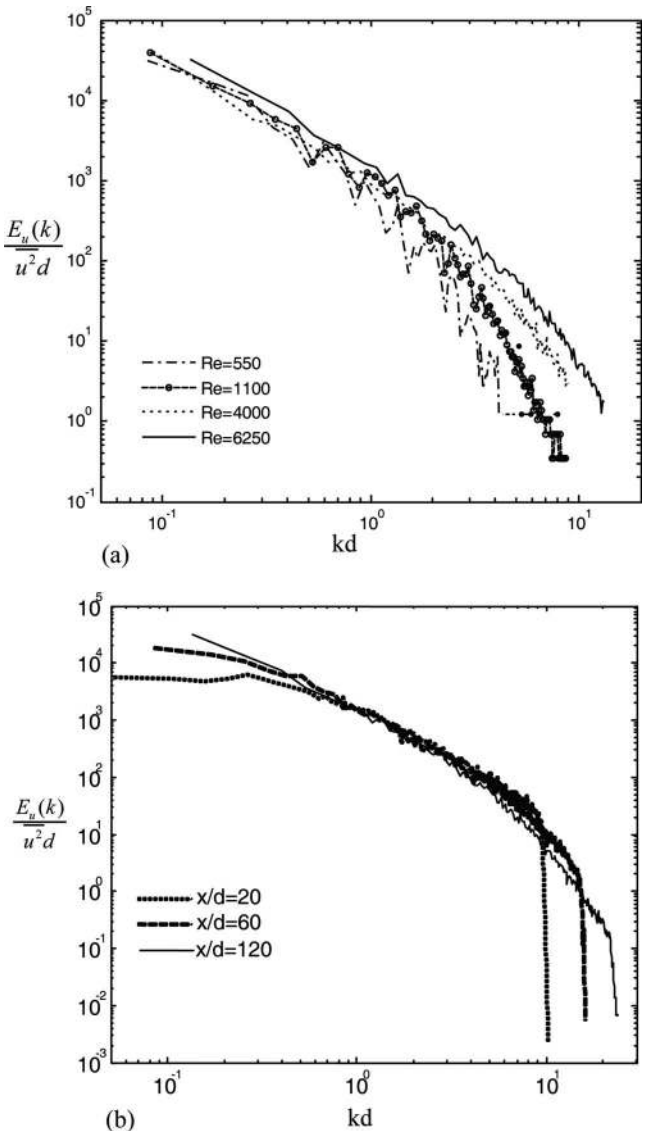

FIG. 17. Variation of wave number spectra. (a) With Reynolds number ($x/d=120$); (b) with axial location (Re=6250).

ergy cascading process can be understood by plotting the power spectrum of velocity fluctuations E_u at different Reynolds numbers and axial locations [Figs. 17(a) and 17(b)]. E_u is defined by the relation

$$\int_0^\infty E_u(k)dk = \overline{u^2}, \tag{3}$$

where the wave number k is given by

$$k = \frac{2\pi f}{U}. \tag{4}$$

Figure 17(a) shows the Reynolds number dependence of wave number spectra at an axial distance of $x/d=120$. It is clear that at this location, the power spectrum broadens with the increase in Re toward higher wave numbers. As a result of this, smaller scales start to appear in the flow at higher Re. Normalized E_u is plotted against wave number at different locations for Reynolds number of 6250 in Fig. 17(b). It is observed that the spectra at locations $x/d=20$, 60, and 120 collapse to one curve in the intermediate range of wave numbers. In fact, location dependence is observed only at lower and higher wave numbers, corresponding to very large or very small eddies. As distance increases, the spectrum broadens, indicating the appearance of finer scales. This is in general agreement with the findings of Huang and Ho[25] and Peacock *et al.*[26]

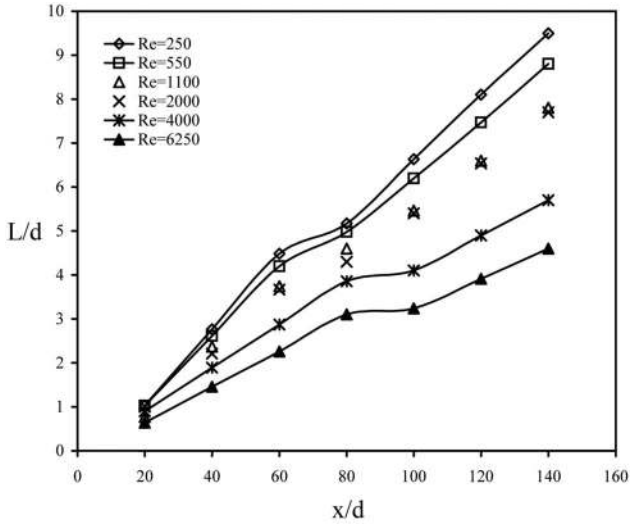

FIG. 18. Variation of integral length scale in the axial direction.

Autocorrelation functions were obtained from the measured data at different locations using a MATLAB program, for estimating the integral time scale τ. The integral length scale at different axial locations is estimated using the Taylor's frozen theory of turbulence[27] as

$$L = U\tau. \tag{5}$$

The integral length scale L thus obtained represents the typical size of energy containing turbulent eddies. In Fig. 18, the integral length scale is observed to increase with respect to axial distance for all the Reynolds numbers of the present study. Length scale decreases with the increase in Reynolds number at a given axial location. This implies that turbulent scales become finer at higher Re values, although a broad range of eddy sizes will coexist at any location. One can conclude that the slower spread rate and centerline decay rate of high Re jets are associated with the reduction of size and strength of the energy containing eddies which are primarily responsible for turbulent mixing in jets. The larger sizes of the integral length scales seen for low Re jets can be attributed to the shear layer instability and the associated large vortices (Figs. 7 and 8). The changes in the slope of the curves in Fig. 18 may be related to the transition from the plane jet to axisymmetric jet spreading behavior. Such transition starts at $x/d=100$ for Re=4000 and 6250, and it starts at $x/d=60$ for low Re values of 250 and 550. This trend is also in accordance with the changes seen in centerline velocity decay for low Re jets.

As the axial distance increases, the local Re increases,[17] implying that the relative significance of viscosity reduces especially for high Re jets in the far field. Consequently, the value of dissipation tends to decrease. The variations of di-

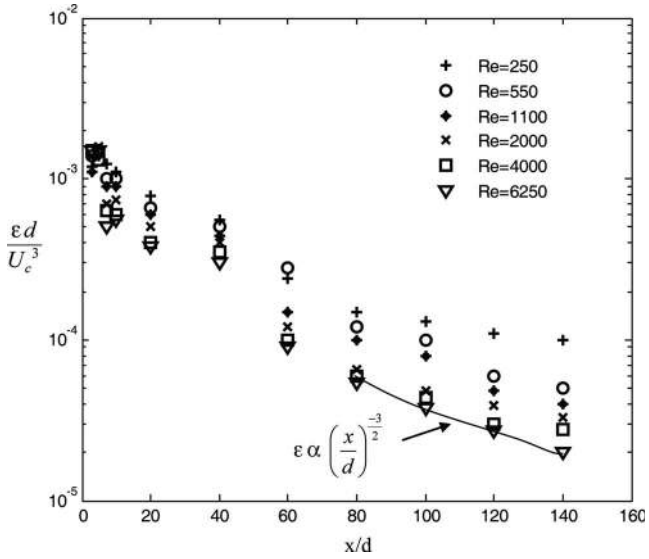

FIG. 19. Variation of dissipation along the axis.

mensionless turbulent kinetic energy dissipation $\varepsilon d/U_c^3$ (where ε is the turbulent kinetic energy dissipation in m^2/s^3) at different x/d positions and various Reynolds numbers are plotted in Fig. 19. In the near region, the value of $\varepsilon d/U_c^3$ is observed to be high. Larger value of dissipation at the jet inlet implies nearly laminar conditions. Away from the nozzle exit, the dimensionless turbulence dissipation rate decreases at higher Re; correspondingly, the value of small scale turbulence production of $\frac{1}{2}(u^2+v^2+w^2)$ is expected to increase due to the decay of large eddies, where v and w are fluctuating velocity components perpendicular to the jet axis. The dissipation decreases with an increase in distance. This also illustrates the fact that smaller structures dominate in the far field which are responsible for lower mixing in high Re jet flows. The far region at high Re obeys the well known trend of $\varepsilon\alpha\ (x/d)^{-3/2}$.

E. Attainment of homogeneous turbulence

Probability density functions (PDFs) of the normalized axial velocity fluctuations are estimated and plotted at various Reynolds numbers and axial locations in Figs. 20(a) and 20(b). The PDF of velocity fluctuations can be used to assess the attainment of homogeneous turbulence and the existence of nonequilibrium and anisotropic features. In the present case, PDF is plotted at the axial distances of $x/d=10$ and 140, representative of the near field and the far field. A Gaussian curve is included in all the plots to assess the deviation, which is an estimate of nonequilibrium present in the flow. Figure 20(a) shows that at $x/d=10$, the PDF has definite peaks and lengths of the exponential tails are also high for low Re cases (Re=250 and 550). This shows the existence of large coherent structures in the flow. At a high Re of 6250, the PDF is skewed but closer to Gaussian. Therefore, it can be concluded that in the initial region of a rectangular jet, anisotropy exists due to the dominance of large scale structures. In the far region [Fig. 20(b)], the PDF is still skewed for low Re jets (Re=250 and 1100) implying that

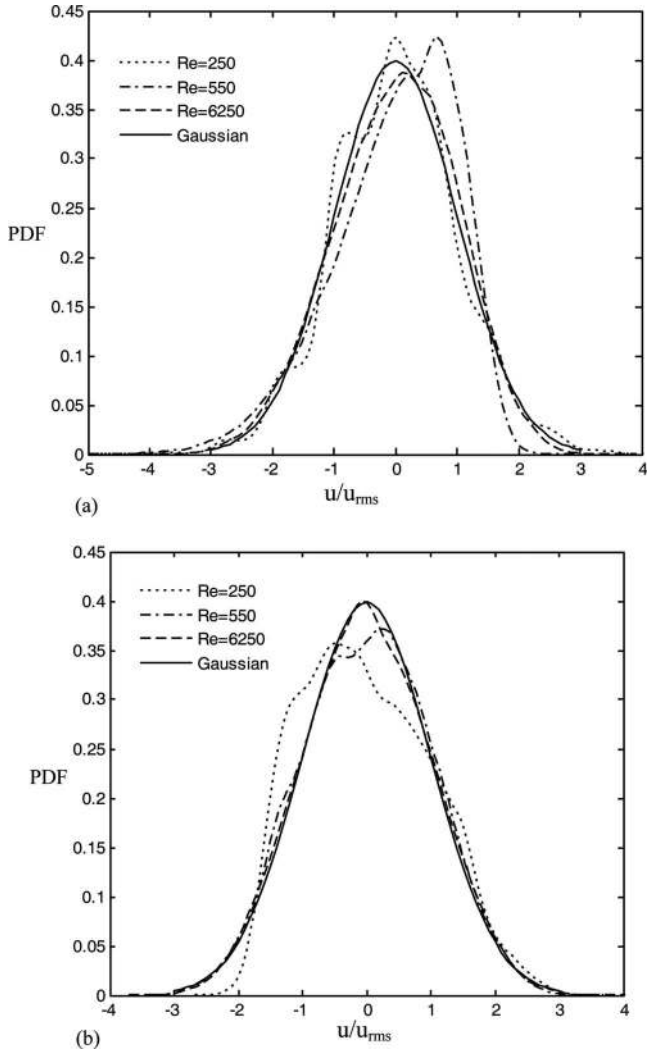

FIG. 20. Probability distribution functions in the near and far regions. (a) $x/d=10$; (b) $x/d=140$.

low Re jets never attain equilibrium turbulence due to the inherent large scale vortices present in the flow. For a high Re jet (Re=6250) at $x/d=140$, the PDF coincides with Gaussian profile indicating that isotropic turbulence has been attained.

IV. CONCLUSIONS

The evolution of mean and fluctuating velocity components in the transition Reynolds number regime of $250 \leqslant Re \leqslant 6250$ has been characterized in detail, for plane free jets. It is found that at lower Reynolds numbers, self-similarity of mean velocity profile is achieved at a smaller axial distance than for the turbulence intensity profile. The near field region of a low Re jet is dominated by discrete frequency peaks due to the vortex shedding associated with shear layer instability. The subsequent vortex pairing processes lead to halving of the fundamental frequency and appearance of other subharmonic components, resulting in the dominance of large size vortices. The flow intermittency associated with large scale vortices persists for a long distance and the flow does not approach an isotropic turbulence con-

dition even in the far field. The spread rate of a low Re jet is high because of the dominance of large size eddies which cause vigorous mixing as well as decay of the jet flow. At higher Reynolds numbers, finer vortex structures dominate the flow. These give rise to slower jet spread rate as well as slower growth of shear layers. Furthermore, the mean velocity and turbulent fluctuations achieve self-similarity almost simultaneously at smaller axial distances. The approach to isotropic turbulence also occurs earlier in a high Re jet.

It is observed that for low Reynolds numbers ($\mathrm{Re} < 2000$), characteristics such as velocity profiles, turbulence intensities, centerline decay rates, and length scales are strong functions of Reynolds number and axial distance. At high Reynolds numbers, the state of turbulence becomes independent of inlet Reynolds number and axial distance, in the far field. For the transitional Reynolds number regime studied here, the overall spread rate of the jet is also strongly influenced by the Reynolds number because of changes in the eddy formation and interaction processes.

[1]L. J. S. Bradbury, "The structure of a self preserving turbulent plane jet," J. Fluid Mech. **23**, 31 (1965).
[2]E. Gutmark and L. Wygnanski, "The planar turbulent jet," J. Fluid Mech. **73**, 465 (1976).
[3]A. D. Weir, D. H. Wood, and P. Bradshaw, "Interacting turbulent shear layers in a plane jet," J. Fluid Mech. **107**, 237 (1981).
[4]L. W. B. Brown, R. A. Antonia, and A. J. Chambers, "The interaction region of a turbulent plane jet," J. Fluid Mech. **149**, 355 (1984).
[5]I. Namer and M. V. Otugen, "Velocity measurements in a plane turbulent air jet at moderate Reynolds numbers," Exp. Fluids **6**, 387 (1988).
[6]A. K. M. F. Hussain, "Coherent structures: Reality and myth," Phys. Fluids **26**, 2816 (1983).
[7]L. P. Bernal and A. Roshko, "Streamwise vortex structure in plane mixing layers," J. Fluid Mech. **170**, 499 (1986).
[8]G. S. Beavers and T. A. Wilson, "Vortex growth in jets," J. Fluid Mech. **44**, 97 (1970).
[9]N. E. Kotsovinos, "A note on the spreading rate and virtual origin of a plane turbulent jet," J. Fluid Mech. **177**, 305 (1976).
[10]J. C. Mumford, "The structures of large eddies in fully developed shear flows. Part 1. The plane jet," J. Fluid Mech. **118**, 241 (1982).
[11]F. O. Thomas and V. W. Goldschmidt, "Structural characteristics of a developing turbulent planar jet," J. Fluid Mech. **163**, 227 (1986).
[12]A. D. Krothapalli, D. Baganoff, and K. Karamcheti, "On the mixing of a rectangular jet," J. Fluid Mech. **107**, 201 (1981).
[13]F. O. Thomas and H. C. Chu, "An experimental investigation of the transition of a plane jet: Subharmonic suppression and upstream feed back," Phys. Fluids A **1**, 1566 (1989).
[14]G. W. Hill, R. C. Jenkins, and B. L. Gilbert, "Effects of the initial boundary layer state on turbulent jet mixing," AIAA J. **14**, 1513 (1976).
[15]A. K. M. F. Hussain and A. R. Clark, "Upstream influence on the near field of a plane turbulent jet," Phys. Fluids **20**, 1416 (1977).
[16]G. Xu and R. A. Antonia, "Effect of different initial conditions on a turbulent round free jet," Exp. Fluids **33**, 677 (2002).
[17]W. K. George, "Role of initial conditions in establishing flow conditions," AIAA J. **42**, 438 (2004).
[18]C. K. W. Tam and T. D. Norum, "Impingement tones of large aspect ratio supersonic rectangular jets," AIAA J. **30**, 304 (1992).
[19]R. J. Moffat, "Contributions to the theory of single-sampled uncertainty analysis," ASME Trans. J. Fluids Eng. **104**, 250 (1982).
[20]H. Sato and F. Sakao, "An experimental investigation of the instability of a two dimensional jet at low Reynolds numbers," J. Fluid Mech. **20**, 337 (1964).
[21]J. Peterson and Y. Bayazitoglu, "Measurements of velocity and turbulence in vertical axisymmetric isothermal and buoyant jets," ASME Trans. J. Heat Transfer **114**, 135 (1992).
[22]I. Wygnanski, "Some measurements in the self preserving jet," J. Fluid Mech. **38**, 577 (1969).
[23]C. K. W. Tam and A. T. Thies, "Instability of rectangular jets," J. Fluid Mech. **248**, 425 (1993).
[24]C. Ho and P. Huerre, "Perturbed free shear layers," Annu. Rev. Fluid Mech. **16**, 365 (1984).
[25]L.-S. Huang and C.-M. Ho, "Small scale transition in a plane mixing layer," J. Fluid Mech. **210**, 475 (1990).
[26]T. Peacock, E. Bradley, J. Hertzberg, and Y.-C. Lee, "Forcing a planar jet flow using MEMS," Exp. Fluids **37**, 22 (2004).
[27]A. A. Townsend, *The Structure of Turbulent Free Shear Flow* (Cambridge University Press, New York, 1976).